

Multisubband theory for the origination of intrinsic oscillations within double-barrier quantum well systems

Peiji Zhao

Department of Electrical and Computer Engineering, North Carolina State University, Raleigh, North Carolina 27695

Dwight L. Woolard

Army Research Laboratory, Army Research Office, Research Triangle Park, North Carolina 27709

H. L. Cui

Department of Physics and Physics Engineering, Stevens Institute of Technology, Hoboken, New Jersey 07030

(Received 26 July 2002; revised manuscript received 4 November 2002; published 21 February 2003)

A theoretical criterion for the origin of high-frequency current oscillations in double-barrier quantum well structures (DBQWS's) is presented. The origin of the current oscillations is traced to the development of a dynamic emitter quantum well (EQW) and the coupling of that EQW to the main quantum well, which is defined by the double-barrier quantum well system. The relationship between the oscillation frequency and the energy-level structure of the system is demonstrated to be $\nu = \Delta E_0/h$. Insight into DBQWS's as potential devices for very high-frequency oscillators is facilitated through two simulation studies. First, a self-consistent, time-dependent Wigner-Poisson numerical investigation is used to reveal sustained current oscillations in an isolated DBQWS-based device. Furthermore, these terahertz-frequency oscillations are shown to be intrinsic. Second a multisubband-based procedure for calculating ΔE_0 , which is the energy separation of the quantum states in the system that are responsible for the instability mechanism, is also presented. Together, these studies establish the fundamental principals and basic design criteria for the future development and implementation of DBQWS-based oscillators. Furthermore, this paper provides physical interpretations of the instability mechanisms and explicit guidance for defining structures that will admit enhanced oscillation characteristics.

DOI: 10.1103/PhysRevB.67.085312

PACS number(s): 73.40.Gk, 72.20.-i

I. INTRODUCTION

The search for compact solid-state based, high-frequency power sources has been an important research subject for many years.¹ Since the end of 1980s, resonant tunneling diodes (RTD's) have been treated as possible high-frequency power sources.² However, as is well known, the traditional implementation of a RTD has not been successful as a power source at terahertz (THz) frequency.³⁻⁵ Indeed, the output power of a RTD is on the order of μ watts at operation frequencies near 1 THz.⁴ This failing is related to the extrinsic design manner of the oscillator that utilizes external circuit elements to induce the oscillation. This failing of the "traditional" RTD-based oscillator is tied directly to the physical principles associated with its implementations. In fact, the f^{-2} law points out that it is impossible to get higher output power at terahertz frequencies for a single device utilized in an extrinsic design manner.² In contrast to the extrinsic design of RTD oscillators, the intrinsic design of RTD oscillators makes use of the microscope instability of RTD's directly.^{3,6} This type of approach will avoid the drawbacks associated with the extrinsic implementation of RTD's. It is believed that if the dynamics surrounding of the intrinsic oscillation can be understood and controlled, RTD sources based on the self-oscillation process should yield milliwatt levels of power in the THz regime.³ However, the exact origin of the intrinsic high-frequency current oscillation has not yet been fully established. The transport dynamics in RTD's is governed by the quantum-mechanical tunneling process that occurs through a quantum well that is formed by a

double-barrier heterostructure. The lack of knowledge related to the origin of the intrinsic instabilities in double-barrier quantum well structures (DBQWS's) directly hampers realizing an optimal design (device and circuit) of a RTD-based oscillator.⁷ Thus, it is extremely important to understand the creation mechanism of the intrinsic instability in DBQWS's.

Historically, Ricco and Azbel suggested in their qualitative arguments that intrinsic oscillation exists in a double-barrier structure for the case of one-dimensional transport.⁸ Their theory attributed the instability to a process that cycled in and out of resonance. Specifically, when the energy of the incoming electrons matched the resonance energy, the tunneling current then charged the potential well and lifted its bottom, thus driving the system away from resonance. The ensuing current decrease (i.e., that associated with the off resonance) then reduced the charge in the well, bringing the system back to resonance, and a new cycle of oscillation commenced. According to such a theory, there should have been current oscillation at the resonance bias. However, numerical simulation results contradict this simple theory.⁹⁻¹¹ In another paper, it was theorized that the nonlinear feedback, caused by stored charges in the quantum well, was responsible for the creation of the current oscillation.¹² However, their phenomenological theory could not explain why the nonlinear feedback caused by stored charge in the quantum well at bias voltages lower than those associated with resonance does not lead to current oscillation.¹¹ In subsequent studies of RTD's, Jensen and Buot observed intrinsic oscillations in their numerical simulations of DBQWS's.⁹

However, this initial work did not provide underlying explanations of the oscillation mechanism. Recently, Woolard *et al.* suggested that the current oscillation might be caused by the charge fluctuation near the emitter barrier of the RTD.¹³ However, the cause of the charge oscillation and how the charge oscillation affects the electronic resonant tunneling were not made clear. Hence, the origin of intrinsic oscillation has eluded revelation for more than a decade. Furthermore, very high-frequency electron dynamics in tunneling structures is of fundamental importance to nanoelectronics. Experimental investigations of similar time-dependent processes are also receiving more attention.^{14,15} However, to date, there has not been a completely conclusive demonstration of intrinsic oscillations in RTD's. Hence, the development of an accurate fundamental theory that provides insight into the catalyst of the intrinsic oscillation is a key first step for the successful design of an RTD-based oscillator.

In earlier work, a theory was presented that provided a basic idea for the origin of the intrinsic oscillation in a DBQWS.¹¹ This theory revealed that the current oscillation, hysteresis, and plateaulike structure in the I - V curve are closely related to the quantum-mechanical wave/particle dual nature of the electrons. In addition, these effects were shown to be a direct consequence of the development and evolution of a dynamical emitter quantum well (EQW), and the ensuing coupling of the quasidiscrete energy levels that are shared between the EQW and the main quantum well MQW formed by the DBQWS. Through this understanding of the dynamical behavior of the RTD, it was possible to qualitatively predict the existence of an oscillation. However, while this initial description was able to self-consistently explain all the physical phenomena related to the intrinsic oscillation it could not provide quantitative design rules. This paper will extend the earlier theory through the application of a basic quantum-mechanical model. A multisubband model for describing the electron dynamics in DBQWS's will be developed. The multisubband-based theory will provide a relationship between the oscillation frequency and the energy-level structure of the system. This subband model will be combined with time-dependent Wigner-Poisson simulation results to provide (i) a quantitative explanation for the origin of the intrinsic oscillations in RTD's, and (ii) a detailed design methodology for future implementation and optimization of DBQWS-based THz oscillators.

This paper is organized as follows. In Sec. II, the fundamental theory for the origin of the intrinsic instability in DBQWS's is developed. Section III is devoted to verify the theory of the origin of intrinsic current oscillation in DBQWS's presented in Sec. II. Numerical experiment results based on the Wigner-Poisson model of quantum devices will be performed. The energy subband structure of the system will be determined by solving a Schrödinger equation. From both numerical calculations, the instability behavior of the system is analyzed, and the underlying mechanisms influencing the intrinsic oscillations are established. In Sec. IV, general conclusions and design rules are given.

II. GENERAL INSTABILITY THEORY FOR MULTISUBBAND SYSTEMS

Previously,¹¹ a qualitative explanation was given for the creation of intrinsic oscillations in a DBQWS. In this prior

work, the oscillations were recognized to arise primarily from two interrelated processes. The first step is the creation of an EQW by quantum interference between the injected and the reflected electron waves. This process dynamically occurs just as the device is being biased into the negative differential resistance (NDR) regime. The intrinsic oscillations are then induced as a secondary result of the coupling between the EQW and the MQW that is defined by the DBQWS. Here, the creation, time-dependent fluctuation, and subsequent disappearance of the EQW are key processes that determine the formation of the I - V characteristics and the intrinsic high-frequency current oscillation. As first revealed in another paper,¹⁶ the intrinsic current-density oscillations result from very small quantum-based fluctuations in potential and are not driven by charge exchange between the EQW and MQW. Here the potential variations within the EQW and MQW are completely in phase, and this indicates that the oscillation is purely of a quantum-mechanical origin.¹⁶

It should be noted that the time-dependent tunneling transport which occurs within the DBQWS is strictly a multisubband transport process once the EQW is created. It is also very important to note that the electron transport under study is occurring within a time-dependent quantum system with dissipation and that this system is subject to open boundary conditions. In this type of situation, strictly speaking, one must consider quasidiscrete electron transport where a density of available tunneling states exist across a continuous energy space. A rigorous analysis would require that a fully time-dependent quantum-mechanical description be applied to derive the peaks of the time-dependent tunneling probability, which could then be used to predict the most probable energy states of the electron dynamics. In other words, the energy levels that we seek to identify cannot be rigorously derived as energy eigenvalues since this is not a proper eigenvalue problem, i.e., the system is open, dissipative, and subject to instability. However, the quasidiscrete energy-level structure can be estimated through an approximate analysis based upon the time-independent Schrödinger's equation. The justification of this approach can be derived as follows. As already stated, the transport problem under study will contain time-dependent potential-energy profiles under some conditions (i.e., when intrinsic oscillations are present) and this profile may be written generally as $U(z,t) = U_0(z) + \Delta U(z,t)$, where the last term contains all the time dependency. As just noted, in this situation most of the electron transport will occur through a set of quasibound resonant energy levels, i.e., defined by the peaks in the transmission function. The wave function associated with each of these subbands may be modeled as

$$\Psi_k(z,t) = e^{(-i/\hbar)F_k(t)} \psi_k(z,t), \quad (1)$$

where $F_k(t) = \int_0^t dt' E_k(t')$, $E_k(t)$ has been defined as the real part of the time-dependent quasibound energy state, and $\psi_k(z,t)$ is the wave-function amplitude. Note that the previous model has been postulated through a modification of the more rigorous relation $\psi_k(z,t) = e^{(-i/\hbar)\int_0^t dt' \hat{H}(z,t')} \psi_k(z,t_0)$, where $\hat{H}(z,t)$ is the system Hamiltonian. Note that the time dependency in ψ_k from Eq. (1) is introduced through dissi-

pation effects (i.e., imaginary energy-state effects). The quasibound system is now described by

$$\begin{aligned}\hat{H}(z,t)\Psi_k(z,t) &= i\hbar \frac{\partial \Psi_k(z,t)}{\partial t} \\ &= \frac{\partial F_k(t)}{\partial t} \Psi_k(z,t) + i\hbar \frac{\Psi_k(z,t)}{\psi_k(z,t)} \frac{\partial \psi_k(t)}{\partial t}.\end{aligned}\quad (2)$$

In the limit of very small time-dependent potential variations, i.e., $\Delta U(z,t) \rightarrow 0$, we must have $\partial \psi_k(z,t)/\partial t \rightarrow 0$, which leads immediately to

$$\hat{H}(z,t)\Psi_k(z,t) = E_k(t)\Psi_k(z,t) \quad (3)$$

since $[\partial F_k(t)]/\partial t = E_k(t)$. Specifically, when the potential variations in time are sufficiently weak then the model coefficients [i.e., $\psi_k(z,t)$] are slowly varying. This allows one to approximate the quasibound energy levels using the time-independent Schrödinger's equation and the time-dependent wave function using Eq. (1). Thus, in this multiple energy-state semiconductor system, the wave function for the electrons can be written generally as

$$\psi(z,t) = \sum_{k=1}^N \Psi_k(z,t). \quad (4)$$

Here, the wave function $\psi_k(z,t)$ is assumed to be independent of the $E_k(t)$. In fact, $\psi_k(z,t)$ can be viewed as the k th subband energy-level coefficient for the total wave function that incorporates effects of dissipative or energy gains induced either by scattering (e.g., electron phonon) or the applied bias source, respectively. For these studies, time variations in $\psi_k(z,t)$ due to either internal dissipation or external energy gains are not on the order of those under consideration (i.e., 10^{12} Hz). Specifically, dissipation effects will not lead to oscillatory behavior that persists and the externally applied biases are time independent. The carrier densities can be easily derived from the subband wave functions as

$$\rho(t) = |\psi(t)|^2. \quad (5)$$

Here, we have suppressed the spatial variables in the expressions of density and wave functions. Substituting Eqs. (4) into (5) yields

$$\begin{aligned}\rho(t) &= |\psi|^2 = \sum_k |\psi_k(t)|^2 \\ &+ 2 \operatorname{Re} \sum_{k,l(l < k)} \psi_k^*(t) \psi_l(t) e^{-i[F_l(t) - F_k(t)/\hbar]}.\end{aligned}\quad (6)$$

The oscillation terms in the above equation will usually be smeared out by the cancellation effect induced by variations in phase (e.g., unequal subband structures leading to conditions such that $E_{l_1} - E_{k_1} \neq E_{l_2} - E_{k_2}$). When these conditions apply the transport can be described simply as an individual summation over single subbands. Hence, there is no coupling

between the bands and no intrinsic oscillations. This is analogous to the more typical transport problem where interband coupling can be ignored and only the first terms in Eq. (6) are necessary. In fact, it is this type of situation where the concept of band transport is most often applied and most useful. However, instability does occur when the system has nonzero coupling and the difference of the subband energies satisfies the following criteria:

- (i) Maximum subband coherence. The energy difference between subbands are equivalent, that is,

$$\Delta E(t) = \Delta E_{lk}(t) = |E_l(t) - E_k(t)| = \text{const}, \quad l \in \{l_i\}, k \in \{k_j\}, \quad (7)$$

where the sets $\{l_i\}$ and $\{k_j\}$ are of equal number and assume all possible values from the number sequences $1, 2, \dots, n$, such as that with $(l_i < k_i)$.

- (ii) Partial subband coherence. A finite and countable number of energy differences are equivalent, that is,

$$\Delta E(t) = \Delta E_{lk}(t) = |E_l - E_k| = \text{const}, \quad l \in \{l_i\}, k \in \{k_j\}, \quad (8)$$

where the sets $\{l_i\}$ and $\{k_j\}$ of equal number, with $(l_i < k_i)$, assume some of the values from the number sequences $1, 2, \dots, n$.

- (iii) Minimum subband coherence. The intrinsic oscillations are characterized by the condition where only a single set of subbands contributes to the instability, that is, $\Delta E(t) = |E_l - E_k|$, where l and k can assume only one set of values from the energy-level index $1, 2, \dots, n$, and $l < k$.

Under these conditions, the carrier density can be written as

$$\rho(t) = |\psi|^2 = \sum_k \langle \psi_k(t) | \psi_k(t) \rangle + 2 \operatorname{Re} \{ e^{-i[\Delta F(t)/\hbar]} G(t) \}, \quad (9)$$

where $\Delta F(t) = \int_0^t dt \Delta E(t)$. The function G , which denotes the coupling between subbands, are slowly varying functions of time and $G \neq 0$, accounting for the nonzero coupling. Here, the incoherent subband terms in Eq. (6) have been excluded. Also while the first terms have been retained, it should be noted that they only contribute to short-term transients and to the final static components of current density and electron density.⁶ The expression defined in Eq. (9) reveals that intrinsic high-frequency oscillations can arise in any quantum system from the wave-function coupling between multisubbands. The instability is specifically achieved *once the subband structure satisfies one of the criteria given above and $G \neq 0$* . Further analysis of the equations can provide a clear physical picture regarding the creation of the oscillation, the main key being the energy-dependent phase factors. It should be noted that prior simulations have shown that the self-consistent potential varies in a periodic form.⁶ Thus, it is reasonable to express the energy difference as

$$\Delta E(t) = \Delta E_0 + f(\omega, t), \quad (10)$$

where $f(\omega, t)$ is a periodic function and ω is the oscillation frequency. ΔE_0 is defined as the average energy difference between two energy levels for a system subject to intrinsic oscillations, or the energy difference at the balance point. Obviously, the phase differences in Eq. (6) between time t_1 and t_2 can be written as

$$\begin{aligned} \Delta \phi(t_1, t_2) &= \frac{1}{\hbar} [\Delta F(t_2) - \Delta F(t_1)] \\ &= \frac{\Delta E_0}{\hbar} (t_2 - t_1) + \frac{1}{\hbar} \int_{t_1}^{t_2} dt' f(\omega, t'). \end{aligned} \quad (11)$$

Recognizing that the phase variation in one period is 2π , the oscillation frequency of electron current, due to the subband structure, is given by

$$\frac{1}{T} = \frac{\Delta E_0}{h}, \quad (12)$$

where T is the period of the intrinsic oscillation. The previous derivation allows us to establish a physics-based description for the creation of the intrinsic oscillation. An accurate physical model for this instability process will be able to describe the time-dependent variations in electron density and potential energy. Consider, for example, an arbitrary oscillation process and assume that the density of electrons at a particular real-space point reaches its maximum value at t_0 . The corresponding potential energy at this same space point will also assume its maximum value at time t_0 since we are considering the Poisson-equation-based interaction potential (i.e., the Hartree approximation to electron-electron interaction). Assuming an oscillation condition exists, this variation in both electron density and electron potential energy will cycle periodically as the phase varies over 2π . The model equation [Eq. (9)] for electron density directly exhibits this type of behavior through the energy-dependent phase factors. In turn, this model would impose variations in the potential energy through the application of Poisson's equation. Most importantly, the feedback influence of potential-energy variations on the energy-dependent phase factor [i.e., defined in Eqs. (10)–(12)] has been incorporated into the analysis.

This quantum-based model allows one to investigate the intrinsic oscillation process to determine the underlying physical mechanisms responsible for the instability. Specifically, if detailed simulations are utilized to derive values for the subband structure and the appropriate ΔE_0 under the condition of intrinsic oscillation then insight into the fundamental catalysts can be obtained. Furthermore, as will be shown later in this paper, this information can be used to predict methods for enhancing the oscillation strength in quantum well systems. The next section of this paper will present simulation tools and studies that allow for a complete analysis of the intrinsic oscillations in DBQWS's. In particular, the Wigner-Poisson-equation-based numerical experiment and the numerical solution of the Schrödinger equation will be used together to derive current-density oscillations, the subband structure, and the subband wave-function amplitudes. This information will be used to verify the fundamental theory of the origin of intrinsic oscillations presented

above and will be used to predict structural modifications that lead to enhanced instabilities in arbitrary quantum well systems.

III. NUMERICAL EXPERIMENT AND INSTABILITY ANALYSIS

It should be noted that, up to date, there are no experimental results regarding the intrinsic instability in DBQWS's, to the best of our knowledge. Thus, it is crucial to employ well-accepted numerical techniques to verify the above-stated instability theory. The above-stated multisubband theory for the origin of current oscillations within DBQWS's shows that the oscillation frequency of the current and energy structure of the system are related in terms of Eq. (12). Thus, this equation can be treated as a criterion for verifying the correctness of the theory. In order to verify the theory, we first did a numerical experiment. The Wigner-Poisson model for quantum devices has been used to describe the transport behavior of carriers in a DBQWS. As will be shown, the results obtained from the Wigner-Poisson transport simulations yield intrinsic current-density oscillations and time-dependent potential-energy profiles. This implies that the energy-level structure must change with the time variation of the double-barrier tunneling structure. Furthermore, if one energy subband exists to conduct the current before the creation of the EQW, there will be at least two energy levels available for passing the current after the creation of the EQW. According to our basic theory, the key to understanding the intrinsic oscillation process is contained within the dynamics of the subband structure after the EQW is created. Hence, direct information regarding the energy structure must be generated to reveal the underlying mechanisms. Thus, numerically solving the Schrödinger's equation in terms of the potential profiles obtained from the numerical experiment, we can get the energy structure of the system at given bias voltages. Comparing the current oscillation frequency obtained from the numerical experiment and that from Eq. (12), the correctness of the theory can be verified. The numerical technique for doing the numerical experiment and solving the Schrödinger's equation for an open system are mature techniques that will not be presented here. Readers can get information about the numerical techniques from our papers and other references.^{9–11,17,18}

Intrinsic current oscillations have been numerically found by several research groups previously.^{9–11} In this paper, for convenience in determining the device structure able to create intrinsic current oscillation, we employ the resonant tunneling structure extensively studied in the literature to verify our instability theory for multiband subband systems.^{9,10} The device parameters used in our simulation are the following. Momentum and position space is broken into 72 and 86 points, respectively. The donor density is 2×10^{18} particles/cm³; the compensation ration for scattering calculations is 0.3; the barrier and well widths are 30 and 50 Å, respectively; the simulation box is 550 Å, the barrier potential is 0.3 eV, corresponding to Al_{0.3}Ga_{0.7}As; the device temperature is 77 K, except that we point out that the effective mass of electrons is assumed to be a constant and equals

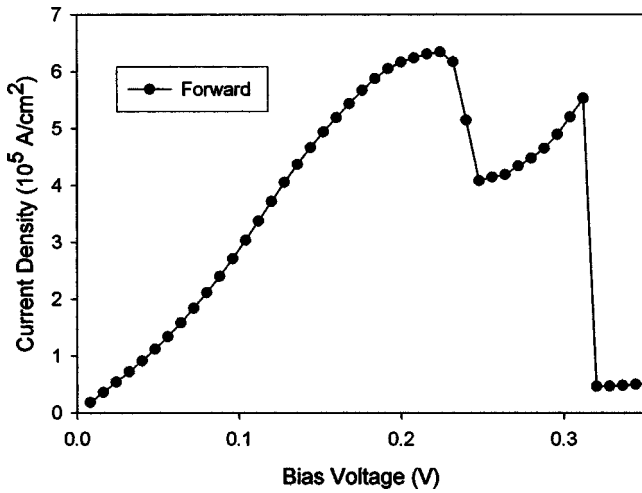


FIG. 1. The current-voltage (I - V) characteristics of the double-barrier quantum well structure (DBQWS) considered in this study.

$0.0667m_0$; the doping extends to 30 \AA before the emitter barrier and after the collector barrier; and the quantum well region is undoped. Bulk GaAs parameters are used to calculate the relaxation time and the chemical potential. The chemical potential is determined by $\int_0^\infty \sqrt{\epsilon} f(\epsilon) d\epsilon = 2/3\mu(T=0)^{3/2}$, where $f(\epsilon)$ is the Fermi distribution function.

Let us first consider simulation results generated from the Wigner-Poisson model of quantum devices. Figure 1 shows the average I - V characteristics for the DBQWS. The I - V characteristic exhibits the plateaulike structure, which has been observed in experimental measurements.¹⁹ It should be noted that instability in the current densities is present within the bias region 0.240 to 0.248 V. Figure 2 plots the current density as a function of time for several values of applied bias. These simulation results exhibit the following important features. First, there is bias voltage window (BVW), defined from 0.240 to 0.248 V, in which the current demonstrates intrinsic oscillations. Second, in the vicinity of the bias voltage point 0.248 V, the current oscillations are stable (i.e.,

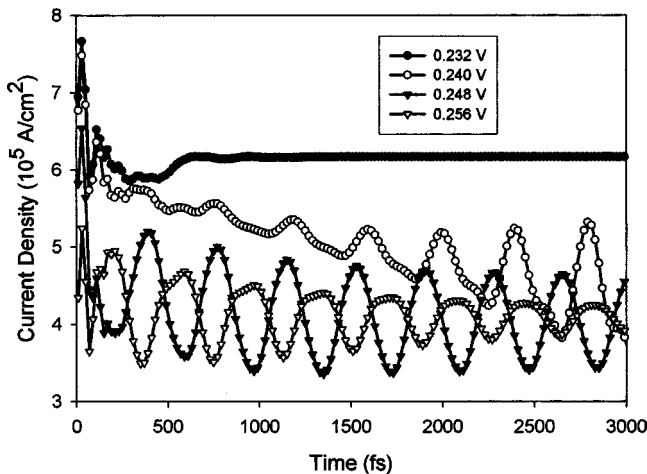


FIG. 2. Current density as a function of time for the DBQWS over the bias voltage window of 0.240–0.248 V. The current oscillation period at 0.248 V is 360 fs.

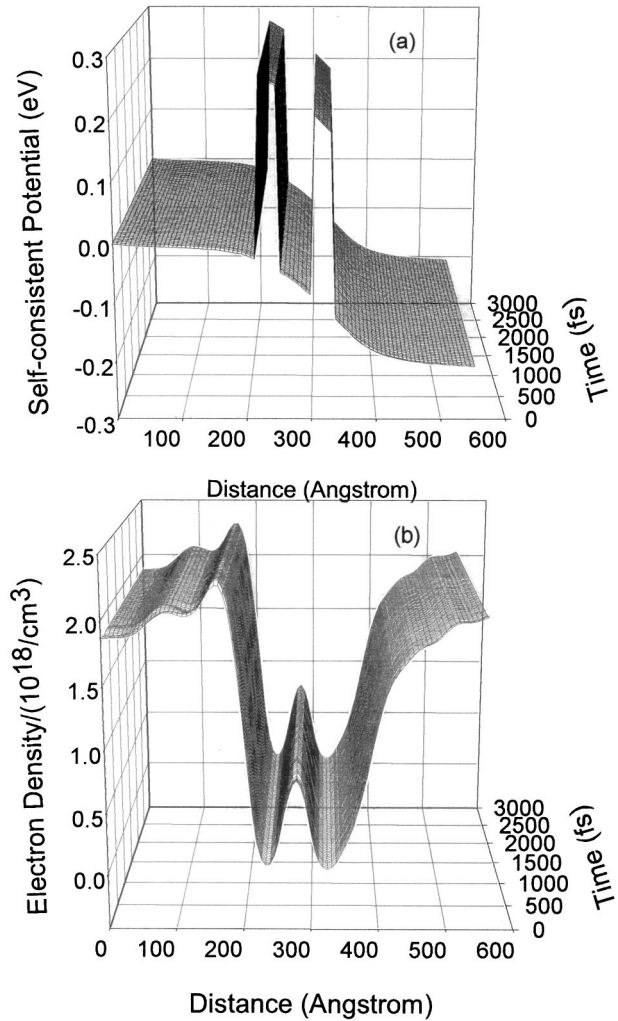


FIG. 3. The time evolution of (a) the electron-density distribution, and (b) the self-consistent potential energy, at a bias voltage of 0.208 V.

they are oscillatory and nondecaying). In our simulation, we have chosen the total simulation time to be 4000 fs. Completely stable oscillations were only observed within a small neighborhood around the bias point 0.248 V. Figures 3–5 show time-dependent self-consistent potential and electron densities at the bias voltages 0.208, 0.248, and 0.296 V, respectively. Collectively, these figures give the potential profiles and electron-density distributions in the BVW and outside the BVW. From these figures it is apparent that the current oscillation in the BVW is concurrent with oscillations of potential and electron densities in the whole region of the device. The oscillations have the following noteworthy features. Before the bias reaches the BVW region (for example, at 0.208 V), the potential and electron densities oscillate for a very short time before settling into a stable state. This feature, which spans a significant region of bias, offers strong evidence against Ricco and Azbel's theory⁸ on the origin of current oscillation in double-barrier systems. In the BVW (at 0.248 V), all the nonperiodic transients of the potential and the electron densities cease after 100 fs. Furthermore, all oscillations are significantly damped outside the

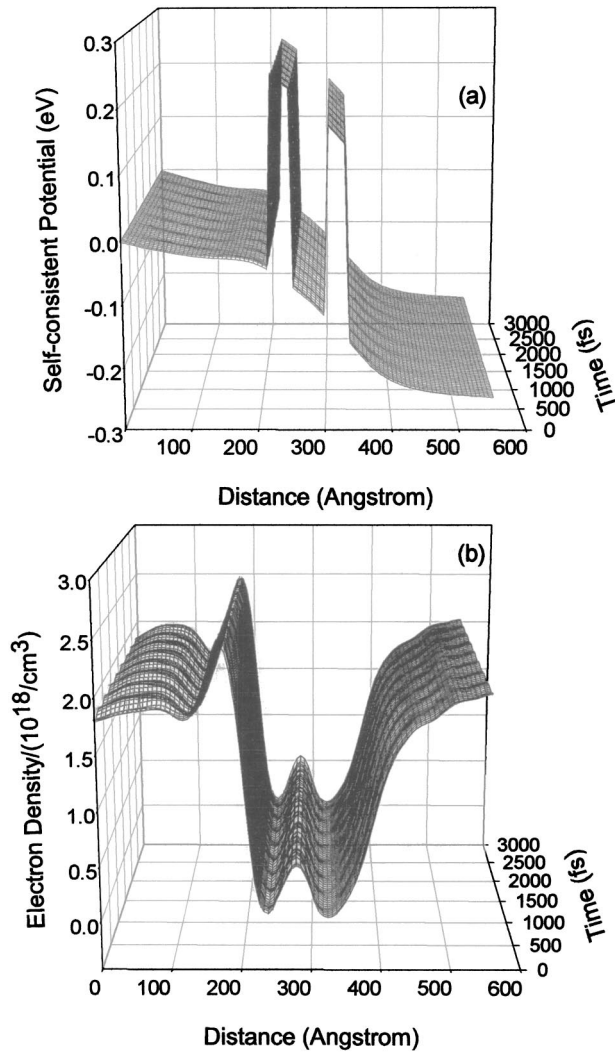


FIG. 4. The time evolution of (a) the electron-density distribution, and (b) the self-consistent potential energy, at a bias voltage of 0.248 V.

BVW (for example, at 0.296 V). The time-dependent results for potential profile and electron density can be used to reveal some of the underlying causes of the intrinsic oscillations in DBQWS's.

The simulation results show that upon entering the BVW an EQW is observed to form in front of the first barrier structure. According to our qualitative and time-dependent quantum energy-level-coupling model, previously given in Ref. 11, the fundamental origin of the intrinsic oscillation can be understood on the following basis. After the bias voltage passes the resonant point, the sudden increase in the electron reflection coefficient associated with the DBQWS leads to a dramatic increase in the amplitude of the reflected electron wave. The interference between the injected and the reflected electron waves causes a large spatial depletion of electron density in the emitter region.²⁰ The depletion of electrons induces a drop in the potential and forms an EQW. Also, the depth of the EQW increases with the increase of the bias voltage, and the energy level of the EQW separates from the three-dimensional states in the emitter region. Fur-

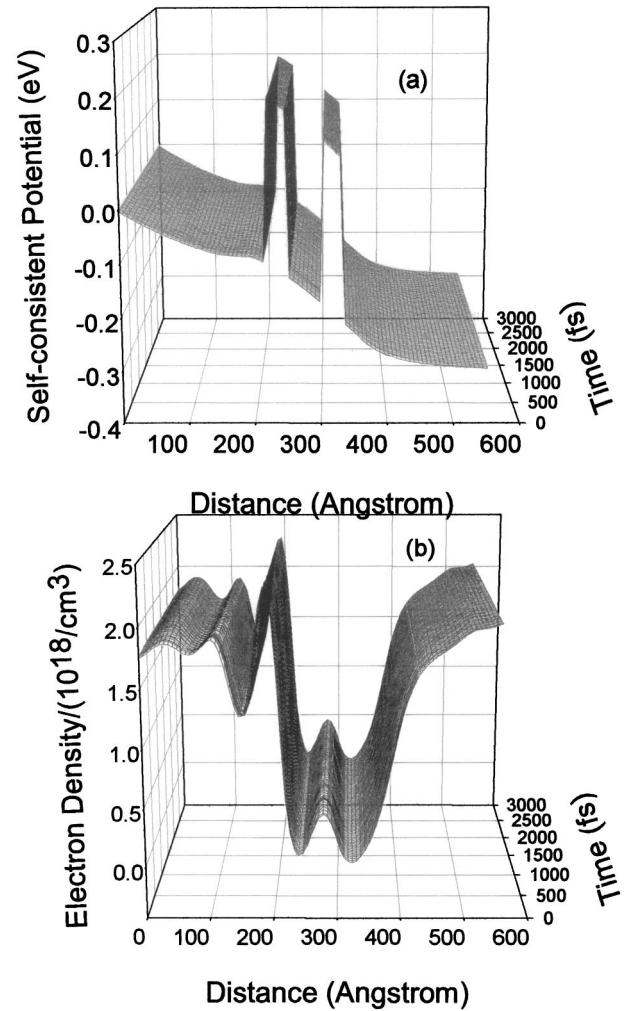


FIG. 5. The time evolution of (a) the electron-density distribution, and (b) the self-consistent potential energy, at a bias voltage of 0.296 V.

thermore, the interaction between the energy level (including the conduction-band edge in the emitter) in the EQW and that in the MQW will greatly influence the transport of electrons through the DBQWS. Several factors jointly influence the tunneling process. The coupling between the conduction-band edge in the EQW and the lowest-energy level in the MQW plays a key role and tends to lift the energy level in the MQW, while at the same time it depresses the conduction-band edge in the EQW. On the other hand, the applied bias has exactly the opposite effect on the energy level in the MQW. The interplay of these two opposite forces determines the existence of the EQW and thereby the major features of the current-time and current-voltage characteristics. These prior arguments, based upon coupling mechanisms between EQW and MQW, provide a qualitative explanation for the origin of the instability. However, a more detailed and indepth investigation is required to establish a robust and quantitative description of the oscillation physics.

As stated in Sec. II, the energy-level structure of the DBQWS and the spatial distribution of the wave function are crucial in determining the origin of the intrinsic current oscillation. Furthermore, Eq. (12) is a criterion in verifying our

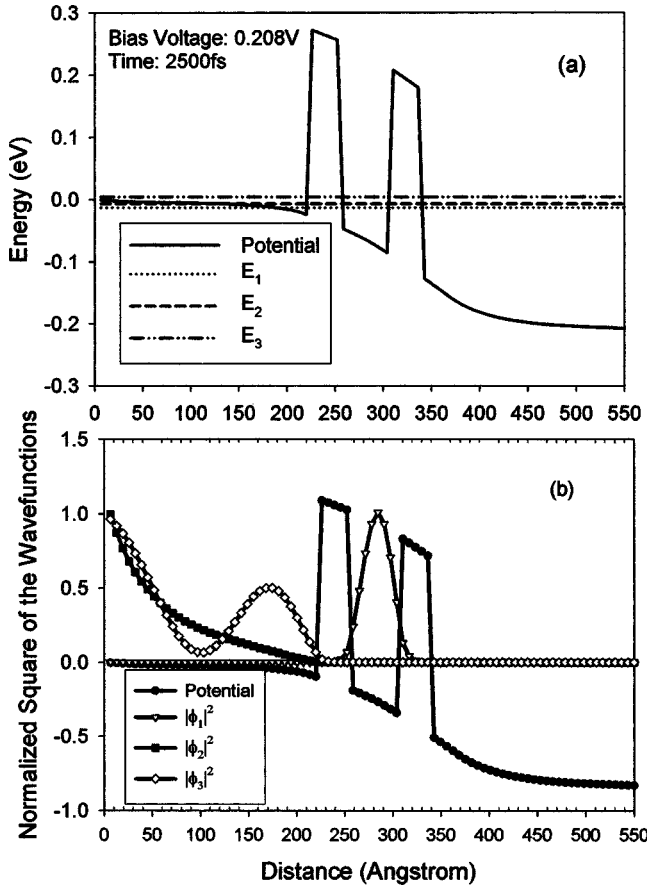


FIG. 6. (a) The energy-subband structure referenced to the potential-energy profile, (b) the square of normalized electron wave functions referenced to the potential-energy profile, both at a bias voltage of 0.208 V and a time of 2500 fs. Since the electrons in E_1 and E_2 are located in different spatial regions, the coupling function $G \sim 0$. Furthermore, since $E_3 > 0$, the lifetime of the state is very short. Thus, the coupling between E_2 and E_3 cannot produce current oscillation.

quantum coupling theory of the origin of the intrinsic oscillation in DBQWS's. Thus, we numerically solved the Schrödinger equation [Eq. (3)].

In solving the Schrödinger equation, the time-dependent potential-energy profiles that were generated by the numerical experiment were utilized. These time-dependent potential profiles can be used to generate time-dependent subband behavior that is approximately consistent (i.e., except for energy-state broadening) with the observed current-density oscillations.

Consider results that correspond to applied biases below the BVW where oscillations are not present. Figure 6(a) shows the time-independent energy-level structure reference to the device conduction-band (CB) profile and Fig. 6(b) gives the square of the wave functions within the DBQWS at bias voltage 0.208 V and at a simulation time where steady-state conditions have been reached (i.e., 2500 fs). Here the subband energy levels are referenced to the energy at the emitter boundary. Though there are two energy levels with negative energies, they do not contribute to the current. Figure 6(b) shows that these two energy states are localized in

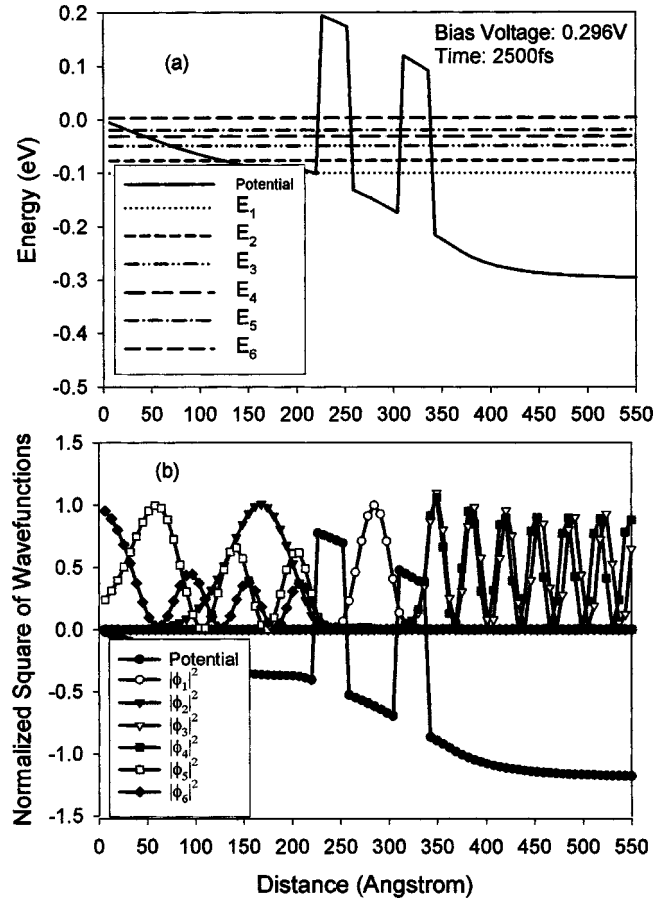


FIG. 7. (a) The energy-subband structure referenced to the potential-energy profile, (b) the square of normalized electron wave functions referenced to the potential-energy profile, both at a bias voltage of 0.296 V and a time of 2500 fs. These figures show that there too many energy subbands in the system. The contributions of the subbands lead to a cancellation effect. Thus, no oscillation can be observed even though the coupling between some subband pairs exists.

different spatial regions. This leads to the fact that the energy-subband coupling function G in Eq. (9) approximates to zero. Thus, the coupling between these two energy levels is neglected. Hence, this subband structure does not meet any of the oscillation criteria as stated in Sec. II. In addition, these results are consistent with the results of Fig. 2 that show no oscillations at a bias voltage of 0.208 V.

Consider next results that correspond to applied biases above the BVW where oscillations are also not predicted by the Wigner-Poisson model. Figure 7 shows the time-independent energy-level structure (again referenced to the device CB profile) and the square of the wave functions within the DBQWS at a bias voltage 0.296 V and simulation time 2500 fs. Here, we see that an EQW has formed due to the presence of significant reflection from the first barrier, and there are six energy levels in the system with negative energies. From Fig. 7 we can see that all energy levels except E_1 may contribute to the oscillation. However, because of the difference of $\Delta E_{ij} = |E_i - E_j|$, the oscillations will be smeared out. Hence, the subband instability criteria are not

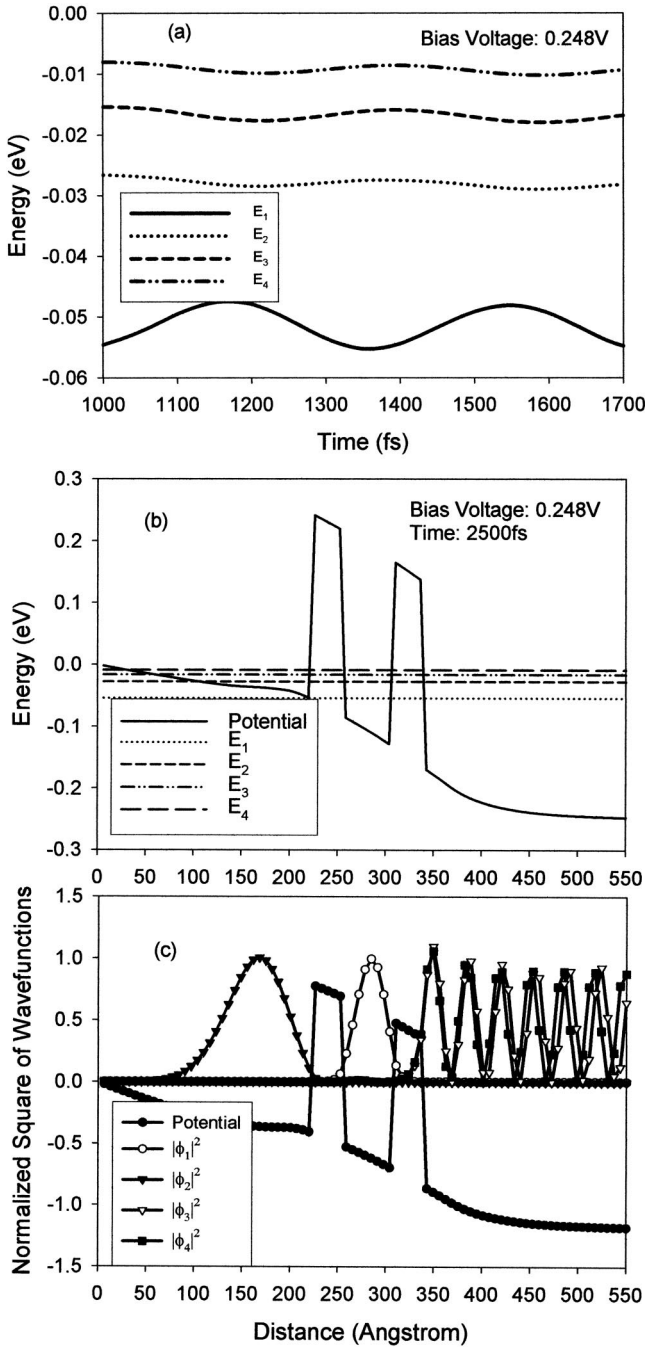


FIG. 8. (a) The time evolution of the energy-subband structure at a bias voltage of 0.248 V. (b) The energy-subband structure referenced to the potential-energy profile, (c) the square of normalized electron wave functions referenced to the potential-energy profile, both at a bias voltage of 0.248 V and a time of 2500 fs. (c) shows that only electrons in E_3 and E_4 are located in the same spatial region thereby having effective coupling. Numerical calculation shows that the widths of E_3 and E_4 are on the order of 10^{-40} . Thus, they are the only subbands able to contribute to the oscillation.

met, and the model predicts no oscillations in agreement with the Wigner-Poisson simulations.

Finally, consider the structure subject to a bias that induces oscillations. Figure 8(a) shows the time-dependent energy-level structure at a bias voltage of 0.248 V. Figure

8(b) gives the energy-level structure (again referenced to the device CB profile) and Fig. 8(c) gives the square of the wave functions of the DBQWS. Results in Figs. 8(b) and 8(c) are for a bias voltage of 0.248 V and a simulation time of 2500 fs. From Figs. 8(b) and 8(c) one can see that there are only two energy levels (E_2 and E_3) that are strongly coupled. These two energy levels contribute to the current oscillation. This case corresponds to that of minimum subband coherence discussed in Sec. II. It is easy to calculate that the average of the energy difference between these two energy levels is 11.07 meV. Thus, Eq. (12) now predicts an intrinsic oscillation frequency of

$$\nu = \frac{1}{T} = 2.68 \text{ THz.} \quad (13)$$

Numerical experiment shows that the oscillation frequency for the current density is 2.8 THz (see Fig. 2). Hence, the quantum energy-level-coupling theory of the origin of intrinsic current oscillation agrees well with the numerical experiment result, with only 4% error of that obtained from numerical experiment, which is based on a complex (and physically complete) simulation model.

The above statements and figures clearly show that there is a BVW in which the current oscillates. For the resonant tunneling structure used in this paper, the BVW is very narrow. This is traced to the creation mechanism of the EQW. With the increase of the bias voltage, the EQW is created after the bias passes the resonance bias voltage. It becomes deeper and deeper with the increase of the bias voltage. In this process, the bias voltage moves into the NDR region and the criteria for creating current oscillation in the device structure are satisfied in a certain bias voltage region, that is, the BVW. Before the bias voltage moves into the BVW, there are not enough subbands within which the electrons in the subbands can sit in a same spatial region and provide the necessary coupling for the creation of the oscillation [see Fig. 6(b)]. After the bias voltage passes the BVW, there are too many subbands that may contribute to the oscillation, resulting in the cancellation effect described in Sec. II. Thus, current oscillations exist only in the BVW. It should be noted that for the device structure used in this paper the BVW sits in the NDR region. This is not appropriate for device application. Our recent research shows that the BVW can be moved to a positive differential resistance region in terms of a careful design of the emitter of the device.²¹

The above analyses verify that the energy-subband coupling and the subband electron distribution in the DBQWS are the key underlying mechanisms for inducing the instability. Moreover, the subband energy-level-coupling model provides basic insight into the phenomenon and offers guidance for defining structures that will admit enhanced oscillation characteristics. These observations will be summarized in the next section.

IV. CONCLUSIONS AND DESIGN CRITERION SUMMARY

In summary, a theory describing the origin of the intrinsic oscillations in a DBQWS has been presented. The relationship between the oscillation frequency and the energy-level

structure of the DBQWS has been established. The theory shows that the quantum-mechanical coupling between the subbands is the root cause of the instability and self-oscillations of the electron density and electron current. Furthermore, the intrinsic oscillations arise directly as a result of the coupling between the energy subbands. Here, the main drivers of the process are the in-phase fluctuations of potential energy within the EQW and MQW that arise out of the subband coupling. Therefore, the instability is a purely quantum-mechanical phenomenon with the frequency of oscillation determined by the average energy difference of the quasidiscrete subband pairs that contribute to the oscillation. These studies establish the fundamental principles for the intrinsic oscillation mechanisms. Most importantly, these studies also provide explicit guidance for defining structures that will admit enhanced oscillation characteristics at operation frequencies within the terahertz regime.

Any practical implementation of a quantum-mechanical-based intrinsic oscillator device to implement a very high-frequency source will require an analysis of the basic device with the embedding circuit. However, these fundamental studies provide important information regarding the design of the resonant tunneling structures that have the capacity for admitting the necessary instability properties. This paper has presented Wigner-Poisson simulation tools for identifying the occurrence of intrinsic oscillations and has developed a simplified subband model for generating the energy-state structure. A summary of the basic design criterion established by these studies include the following:

(i) For certain applied biases the DBQWS develops an EQW that couples to the MQW defined by the double-barrier heterostructures of the resonant tunneling diode. The subband coupling then induces quantum-based fluctuations in the potential-energy profile that lead to intrinsic oscillations in electron density and electron current. Since these oscillations are critically dependent on the coupling of the quasi-discrete energy levels, the intrinsic oscillations will only occur at sufficiently low temperatures (e.g., 77 K) that allow for the formation of a distinct subband structure (minimum-energy broadening effects). Hence, depending on the operation temperature selected, an adequate level of resolvability within the subband structure must be established to enable the instability mechanism.

(ii) The demonstration of the subband coupling as the

underlying catalyst for the intrinsic instability immediately provides guidance for alternative heterostructure systems that should provide superior oscillation performance. For example, in the DBQWS under study the subband coupling develops between the MQW, which always exists, and the EQW that forms only at certain biases due to interference effects arising out of quantum reflections from the first heterostructure barrier. An alternative approach for realizing intrinsic oscillations is to utilize a double-well system constructed from a triple-barrier heterostructure system. This approach will provide more latitude in biasing the device, in that oscillations should be produced over a wider range of applied bias. There is also the possibility that a multiple double-well system may be combined to realize larger oscillation amplitudes. Also, as the fundamental driver of the instability is the subband coupling, it is certainly possible to envision single-well systems that yield coupled subbands (e.g., parabolic wells) with the potential for producing intrinsic oscillations. Finally, as was directly demonstrated by the studies presented here, it is possible to utilize well engineering to modify the shape of the quantum wells and enhance the amplitude of the observed current-density oscillation.

(iii) Since the subband coupling has been shown to produce the instability, it should be possible to design structures that yield enhanced oscillation amplitudes through engineering the energy-level separations and the associated phase of the quantum-mechanical scattering-state functions. Specifically, the theory has demonstrated that the oscillation is a product of individual subband-pair coupling. In particular, results from this study demonstrated a case of minimum subband coherence where only one pair of energy states contributed to the oscillation. Hence, if tunneling structures were designed such that partial or maximum subband coherence was achieved then the amplitude of the current oscillation should be enhanced. This would specifically entail the design of structures that resulted in equal energy-state spacing and coherent coupling of wave functions of the subbands. A general theoretical description of this procedure is given in Sec. II.

ACKNOWLEDGEMENT

We are grateful to Kevin Jensen for providing the RTD simulator for generating the Wigner-Poisson simulation results used in this paper.

¹F. Capasso, F. Beltram, S. Sen, A. Palevski, and A. Y. Cho, in *High Speed Heterostructure Devices*, edited by R. A. Kiehl and T. C. L. G. Sollner (Academic, New York, 1994); A. Tredieucci *et al.*, *Electron. Lett.* **36**, 876 (2000); H. Eisele *et al.*, *IEEE MTT-S Int. Microwave Symp. Dig.* **48**, 626 (2000); J. M. Chamberlain, in *New Directions in Terahertz Technology*, edited by J. M. Chamberlain and R. E. Miles (Kluwer, Dordrecht, 1997).

²T. C. L. G. Sollner *et al.*, *Appl. Phys. Lett.* **50**, 332 (1984); E. R. Brown, in *Hot Carriers in Semiconductor Nanostructures*, edited by J. Shah (Academic, Boston, 1992) pp. 469; E. Lheurette *et al.*, *Electron. Lett.* **28**, 937 (1992).

³D. L. Woolard *et al.*, *53rd Annual Device Research Conference Digest* (IEEE, Inc., Piscataway, NJ, 1995), p. 54.

⁴O. Boric-Lubecke *et al.*, *IEEE MTT-S Int. Microwave Symp. Dig.* **43**, 969 (1995).

⁵C. Kidner *et al.*, *IEEE MTT-S Int. Microwave Symp. Dig.* **38**, 864 (1990).

⁶Peiji Zhao *et al.*, *Very Large Scale Integrated Design* (2001), Vol. 13, p. 413.

⁷D. L. Woolard *et al.*, *IEEE Trans. Educ.* **43**, 332 (1996).

⁸B. Ricco and M. Ya. Azbel, *Phys. Rev. B* **29**, 1970 (1984).

⁹K. L. Jensen and F. A. Buot, *Phys. Rev. Lett.* **66**, 1078 (1991).

- ¹⁰B. A. Biegel and J. D. Plummer, *Phys. Rev. B* **54**, 8070 (1996).
- ¹¹Peiji Zhao, H. L. Cui, and D. Woolard, *Phys. Rev. B* **63**, 075302 (2001).
- ¹²C. Presilla *et al.*, *Phys. Rev. B* **43**, 5200 (1991).
- ¹³D. L. Woolard *et al.*, *J. Appl. Phys.* **79**, 1515 (1996).
- ¹⁴E. Schombury *et al.*, *Electron. Lett.* **35**, 1419 (1999); K. Kofbeck *et al.*, *IEEE Microwave Guid. Wave Lett.* **8**, 427 (1990).
- ¹⁵N. C. Kluksdahl *et al.*, *Phys. Rev. B* **39**, 7720 (1988).
- ¹⁶Dwight Woolard, Peiji Zhao, and H. L. Cui, *Physica B* **314**, 108 (2002).
- ¹⁷W. R. Frensley, *Superlattices Microstruct.* **11**, 347 (1992).
- ¹⁸Y. X. Liu, D. Z.-Y. Ting, and T. C. McGill, *Phys. Rev. B* **54**, 5675 (1996).
- ¹⁹V. J. Goldman *et al.*, *Phys. Rev. Lett.* **58**, 1256 (1987).
- ²⁰Peiji Zhao, H. L. Cui, and D. Woolard, *J. Appl. Phys.* **87**, 1337 (2000).
- ²¹Peiji Zhao, D. Woolard, and H. L. Cui (unpublished).